Jpn. J. Appl. Phys. Vol. 42 (2003) pp. 4659–4662
Part 1, No. 7B, July 2003

Si(111)-$\sqrt{21} \times \sqrt{21}$-(Ag+Cs) Surface Studied by Scanning Tunneling Microscopy and Angle-Resolved Photoemission Spectroscopy

Canhua LIU, Iwao MATSUDA, Harumo MORIKAWA, Hiroyuki OKINO, Taichi OKUDA[1], Toyohiko KINOSHITA[1] and Shuji HASEGAWA

Department of Physics, School of Science, University of Tokyo, 7-3-1 Hongo, Bunkyo-ku, Tokyo 113-0033, Japan
[1]*Synchrotron Radiation Laboratory, Institute of Solid State Physics, University of Tokyo, 5-1-5 Kashiwanoha, Kashiwa, Chiba 277-8581, Japan*

(Received October 30, 2002; accepted for publication December 18, 2002)

Scanning tunneling microscopy (STM) and angle-resolved photoemission spectroscopy (ARPES) were used to study the atomic and electronic structures of the Si(111)-$\sqrt{21} \times \sqrt{21}$-(Ag+Cs) surface ($\sqrt{21}$-Cs in short), which was induced by depositing caesium atoms on the Si(111)-$\sqrt{3} \times \sqrt{3}$-Ag surface at room temperature (RT). Compared with previously reported STM images of noble-metal induced $\sqrt{21} \times \sqrt{21}$ phases including the Si(111)-$\sqrt{21} \times \sqrt{21}$-(Ag+Ag) and Si(111)-$\sqrt{21} \times \sqrt{21}$-(Ag+Au) surfaces ($\sqrt{21}$-Ag and $\sqrt{21}$-Au, respectively), the $\sqrt{21}$-Cs surface displayed quite different features in STM images. The ARPES data of the $\sqrt{21}$-Cs surface revealed an intrinsic dispersive surface-state band, together with a non-dispersive one near the Fermi level, which was also different from those of the $\sqrt{21}$-Ag and $\sqrt{21}$-Au surfaces. These results strongly suggest different atomic arrangements between Cs- and noble-metal induced $\sqrt{21} \times \sqrt{21}$ phases. Unlike the $\sqrt{21}$-Ag and $\sqrt{21}$-Au phases, the framework of the initial Si(111)-$\sqrt{3} \times \sqrt{3}$-Ag substrate is totally broken at the $\sqrt{21}$-Cs phase. [DOI: 10.1143/JJAP.42.4659]

KEYWORDS: scanning tunneling microscopy, angle-resolved photoemission spectroscopy, Si(111), surface superstructure

1. Introduction

The atomic arrangement and electronic structure of binary metal adsorbates on a Si(111) surface have recently attracted considerable attention from fundamental and technological points of view. Since Nogami *et al.* and Ichimiya *et al.* independently found that Au adsorbates on the Si(111)-$\sqrt{3} \times \sqrt{3}$-Ag surface at room temperature (RT) form an ordered superstructure with $\sqrt{21} \times \sqrt{21} \pm \mathrm{R}10.9^\circ$ periodicity ($\sqrt{21}$-Au in short hereafter),[1,2] the $\sqrt{21} \times \sqrt{21}$ phase was extensively studied by scanning tunneling microscopy (STM), photoemission spectroscopy and surface X-ray diffraction.[3,4] In addition to Au adsorption at RT, Cu (at RT) and Ag (at low temperature, LT) adsorptions have also been found to form the surface phases of $\sqrt{21} \times \sqrt{21}$.[5–8] All three kinds of noble metals are now known to induce the $\sqrt{21} \times \sqrt{21}$ surface phases which show quite similar patterns of reflection-high-energy electron diffraction (RHEED) and low-energy-electron diffraction (LEED); they show double domains of $\sqrt{21} \times \sqrt{21}$ with $\pm 10.89^\circ$ orientations with respect to $[11\bar{2}]$ crystal orientation. In particular, the Ag- and Au-induced $\sqrt{21} \times \sqrt{21}$ surface phases are found to exhibit very similar STM images, and thus are considered to have quite similar atomic arrangements.[8] Several models of the atomic structure of $\sqrt{21} \times \sqrt{21}$ phases have been proposed based on the STM and X-ray diffraction investigations, all of which assume that the framework of the under-layer structure of the Si(111)-$\sqrt{3} \times \sqrt{3}$-Ag surface is not basically broken by adsorption of Ag or Au adatoms.[1,2,4,6]

Since the $\sqrt{21} \times \sqrt{21}$ surface phases were found to have a very high surface electrical conductivity several years ago,[9–11] their surface electronic structures were carefully investigated.[3,7] The $\sqrt{21}$-Ag and $\sqrt{21}$-Au phases have similar surface-state bands, which are also similar to those of the initial Si(111)-$\sqrt{3} \times \sqrt{3}$-Ag phase, though some additional bands appear by Au adatom adsoprtion. This is one of the reasons why the adatoms sit on a basically unaltered Si(111)-$\sqrt{3} \times \sqrt{3}$-Ag surface, and why the $\sqrt{21}$-Ag and $\sqrt{21}$-Au have quite similar atomic structures. It is also considered that there is no covalent-like bonding between the adatoms and substrate, so that the adatoms are very mobile on the substrate.[6] A major change in the surface-state bands caused by Ag or Au adatom adsorption is that they shift in energy position toward higher binding energy. This is due to electron transfer from the Ag or Au adatoms into a surface-state band (called S_1 state) of the Si(111)-$\sqrt{3} \times \sqrt{3}$-Ag substrate.[7] This is electron doping into a surface-state band by adsorbates.[12] The high surface conductivity of the noble-metal induced $\sqrt{21} \times \sqrt{21}$ phases is mainly due to the deepened metallic surface-state and the resulting enlarged Fermi disc of the initial Si(111)-$\sqrt{3} \times \sqrt{3}$-Ag surface.

In recent years, it has been found that alkali metals including Cs adsorbates on the Si(111)-$\sqrt{3} \times \sqrt{3}$-Ag surface can also induce $\sqrt{21} \times \sqrt{21}$ phases, which show similar high surface conductivity that shown by the $\sqrt{21}$-Ag and $\sqrt{21}$-Au phases.[5] Because of monovalency of these adatoms for inducing the $\sqrt{21} \times \sqrt{21}$ phases, it is expected that the atomic and electronic structure of the $\sqrt{21}$-Cs phase is also similar to those of the $\sqrt{21}$-Ag and $\sqrt{21}$-Au phases. In this study we investigate the atomic arrangement and electronic structure of the surface phase of $\sqrt{21}$-Cs for the first time. Contrary to expectations, the $\sqrt{21}$-Cs phase was found to be quite different from the $\sqrt{21}$-Ag and $\sqrt{21}$-Au phases in atomic and electronic structures.

2. Experiment

The experiments were conducted in two separate ultrahigh vacuum (UHV) chambers, one of which was for LT-STM (UNISOKU-USM 501), and the other was for angle-resolved photoemission spectroscopy (ARPES, VG-ADES 500). The latter was on BL-18A (Institute of Solid State Physics, University of Tokyo) at Photon Factory of KEK in Tsukuba, Japan. The substrate was a P-doped *n*-type Si(111) wafer with resistivity of 2–15 Ω·cm at RT, and its typical dimensions were $15 \times 3 \times 0.4\,\mathrm{mm}^3$ for the LT-STM experiment and $25 \times 5 \times 0.4\,\mathrm{mm}^3$ for the ARPES experiment.

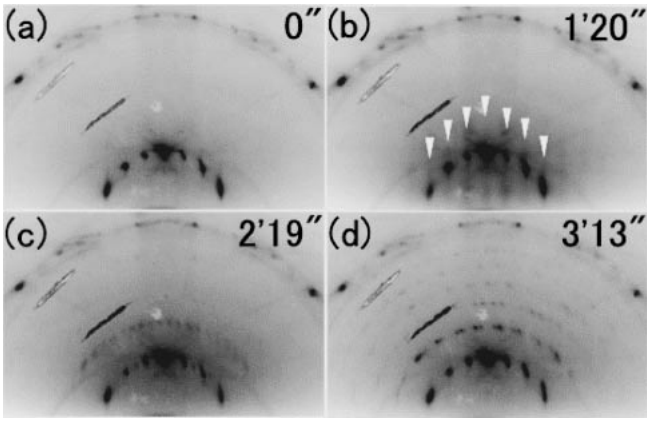

Fig. 1. RHEED patterns observed at RT during Cs evaporation. The number at the top-right corner in each figure is the Cs evaporation time. (a) The initial Si(111)-$\sqrt{3} \times \sqrt{3}$-Ag surface before Cs adsorption. (b) At 1 min and 20 s of Cs deposition. (c) At 2 min and 20 s. The Si(111)-6 × 6-(Ag+Cs) surface emerged. (d)The Si(111)-$\sqrt{21} \times \sqrt{21}$-(Ag+Cs) structure was formed by evaporating Cs at around 3 min.

In the LT-STM experiment, a clear 7 × 7 RHEED pattern was produced by flashing the sample at 1200°C several times by passing a direct current of about 10 A through it in vacuum of 10^{-10} Torr range. The Si(111)-$\sqrt{3} \times \sqrt{3}$-Ag structure was formed at a substrate temperature of ~520°C by depositing just one monolayer of Ag atoms. It was confirmed by observing the change of RHEED pattern during the deposition as shown in Fig. 1(a). Then, the wafer was cooled to RT, and Cs atoms were evaporated from a thoroughly out-gassed commercial dispenser (SAES Getters Inc.) until a clear $\sqrt{21} \times \sqrt{21}$ RHEED pattern emerged as shown in Fig. 1(d). After the confirmation of the $\sqrt{21}$-Cs RHEED pattern, the sample was swiftly transferred to a cold STM stage where it was cooled to 70 K. An electrochemically sharpened Tungsten tip was used for STM. STM observations at LT were better than at RT due to structural stability because Cs atoms are mobile on the substrate at RT. Such mobility of Cs atoms at RT, however, is required to form the $\sqrt{21}$-Cs phase with large domains.

For the ARPES experiment, similar procedures were followed for the sample preparation with the help of LEED instead of RHEED. The sample was cooled to 120 K for obtaining the spectra for the same reason. The temperature difference between 120 K at ARPES and 70 K at STM should not cause any essential change in the structure of the $\sqrt{21}$-Cs phase according to RHEED and LEED inspections. The ARPES spectra were measured using linearly polarized synchrotron radiation with photon energy of 21.2 eV. The overall angular and energy resolutions were about 1.5° and 0.1 eV, respectively. According to changes of work function measured by photoemission as a function of Cs coverage, the strongest $\sqrt{21}$-Cs LEED pattern was observed at Cs coverage which was slightly more than that at the minimum work function.

3. Results and Discussions

Figures 1(a)–1(d) are a series of RHEED patterns taken during Cs deposition; (a) is the initial substrate, Si(111)-$\sqrt{3} \times \sqrt{3}$-Ag, taken at RT just before Cs deposition. After evaporating Cs for about 1 min and 20 s, there emerged broad streaks indicated by arrowheads in Fig. 1(b). Since 6 × 6 spots appeared by further deposition of Cs as shown in Fig. 1(c), the streaks in (b) were considered to be a kind of precursory state of short-range ordered 6 × 6 domains. It should be noted here that no 6 × 6 phase appears before the $\sqrt{21} \times \sqrt{21}$ phases are formed for the cases of noble-metal adsorptions. After evaporating Cs for about 3 min, RHEED spots of the $\sqrt{21}$-Cs were observed to be the strongest as shown in Fig. 1(d). Even with further Cs deposition at RT, the RHEED pattern of $\sqrt{21}$-Cs phase hardly changed.

Figure 2(a) shows an STM image of the $\sqrt{21}$-Cs surface at 70 K. Letters *A* and *B* in the figure indicate two domains whose unit cells are denoted by two quadrangles rotated at 21.78° with respect to each other. Such large domains of the $\sqrt{21}$-Cs structure produce the sharp RHEED spots as shown in Fig. 1(d). Figures 2(b)–2(g) are magnified STM images of the $\sqrt{21}$-Cs phase; Figs. 2(b)–2(d) are filled-state images,

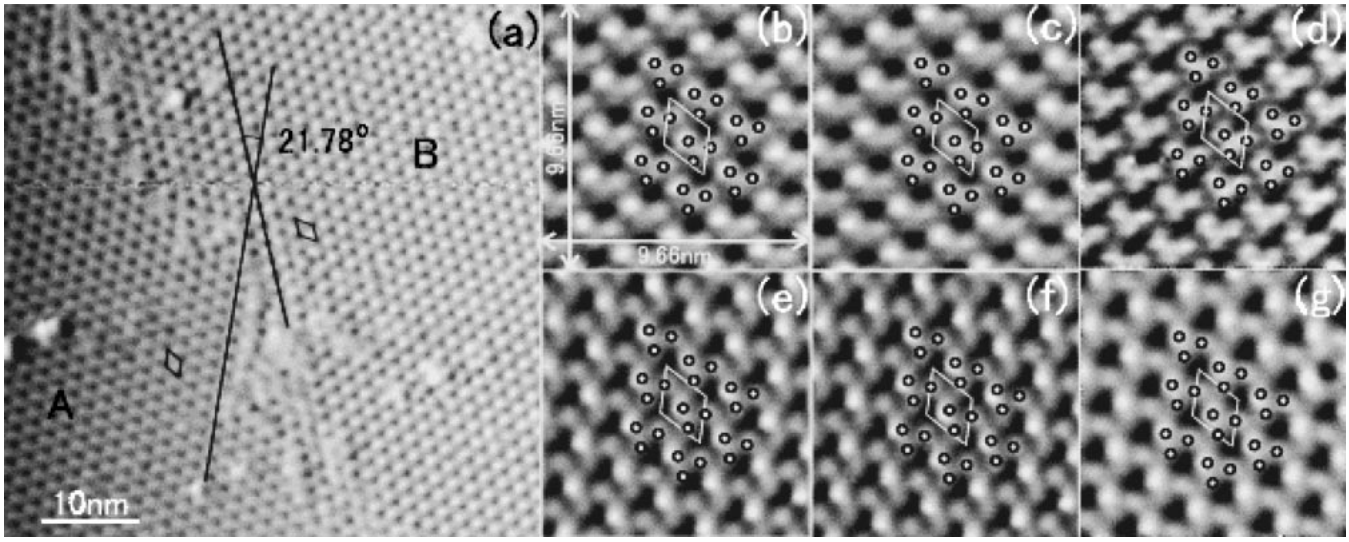

Fig. 2. STM images of the Si(111)-$\sqrt{21} \times \sqrt{21}$-(Ag+Cs) surface taken at about 70 K under constant-height mode, (a) STM image with $V_t = 1.0$ V and $I_t = 0.75$ nA. (b)–(g) Enlarged STM images with $I_t = 0.75$ nA and different tip bias: (b) $V_t = 0.05$ V. (c) $V_t = 0.1$ V. (d) $V_t = 0.5$ V. (e) $V_t = -0.05$ V. (f) $V_t = -0.1$ V. (g) $V_t = -0.2$ V.

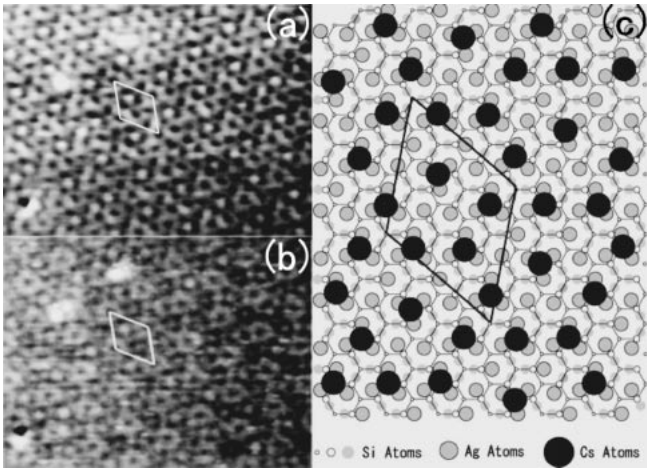

Fig. 3. STM images of the Si(111)-$\sqrt{21} \times \sqrt{21}$-(Ag+Au) surface, taken at RT with $I_t = 0.5$ nA. (a) Filled-state image with $V_t = 0.5$ V. (b) Empty-state image with $V_t = -0.5$ V. (c) A possible surface structure model proposed by Nogami *et al.*[1)]

and Figs. 2(e)–2(g) are empty-state ones. In all images, unit cells are indicated by white quadrangles. Namely, that there are basically three protrusion spots in the unit cell in both filled- and empty-state images as denoted by small circles. Although they do not appear to be completely the same, all of the protrusion maxima locate at the same position in all images.

In order to compare the images of the $\sqrt{21}$-Cs phase with those of noble-metal induced $\sqrt{21} \times \sqrt{21}$ phases, the surface of $\sqrt{21}$-Au was observed again by our STM at RT with better resolution than in the previous studies.[1,2)] Figure 3 shows filled- and empty-state STM images of the $\sqrt{21}$-Au surface. Protrusions are located in the same position in both images. Tong *et al.* have reported LT-STM images of the $\sqrt{21}$-Ag surface,[7)] which were quite similar to the images of the $\sqrt{21}$-Au surface. Based on these STM images, models of the atomic arrangements of these $\sqrt{21} \times \sqrt{21}$ phases are proposed, one of which is shown in Fig. 3(c) proposed by Nogami, *et al.*[1)] In the model, the substrate of the Si(111)-$\sqrt{3} \times \sqrt{3}$-Ag structure is assumed to be unaltered, for which the honeycomb-chained-triangle model[13)] is used. All the additional Au adatoms locate on the centre of Ag triangles and are arranged periodically according to the protrusions in STM images. The protrusions in STM images of $\sqrt{21}$-Cs phase in Figs. 2(b)–2(g) look quite different from those of the $\sqrt{21}$-Au phase in Fig. 3. Thus we come to the conclusion that the atomic structure of the $\sqrt{21}$-Cs phase is quite different from that of the $\sqrt{21}$-Ag and $\sqrt{21}$-Au surfaces.

Figure 4(a) contains ARPES spectra for the $\sqrt{21}$-Cs surface taken at 120 K, and Fig. 4(b) is its grey-scale band-dispersion diagram constructed from the second-derivatives of the spectra (a) by using the measured work function of 2.53 eV. It is very clear that there are two surface state bands near the Fermi level; S_1 is almost at Fermi energy without dispersion while S_2 is dispersing upwards crossing the Fermi level. The bottom of S_2 band is located in between the $\bar{\Gamma}$ and $\bar{M}$ points in the second $\sqrt{3} \times \sqrt{3}$-surface Brillouin zone (SBZ).

The electronic structures of both the $\sqrt{21}$-Ag and $\sqrt{21}$-Au surfaces have been studied carefully,[3,7)] and it is reported that in both surfaces, there is a metallic surface-state band named S_1^* dispersing around the $\bar{\Gamma}$ point of the second SBZ of $\sqrt{3} \times \sqrt{3}$ superstructure (at 1.09 Å^{-1} on the wave number $k_\parallel$ axis). Theoretical calculation suggests that the S_1^* surface state originates from the original S_1 state of the initial Si(111)-$\sqrt{3} \times \sqrt{3}$-Ag surface;[14)] the S_1 state is downward shifted to be the S_1^* state due to electron transfer from Ag or Au adatoms to the substrate. The S_1^* state mainly obeys the $\sqrt{3} \times \sqrt{3}$ periodicity. This is an important factor supporting the assumption that the under layer of the Si(111)-$\sqrt{3} \times \sqrt{3}$-Ag surface is not altered when the surface structure of $\sqrt{21}$-Ag or $\sqrt{21}$-Au is formed. Since we could not find such bands around $\bar{\Gamma}$ point of the $\sqrt{3} \times \sqrt{3}$ SBZ, the band structure of the $\sqrt{21}$-Cs phase is completely different from those of the $\sqrt{21}$-Ag and $\sqrt{21}$-Au phases. In the band-dispersion diagram of the $\sqrt{21}$-Cs phase, there seemed no date showing the surface states of the Si(111)-$\sqrt{3} \times \sqrt{3}$-Ag surface remaining. This means that the framework of the Si(111)-$\sqrt{3} \times \sqrt{3}$-Ag under-layer is basically broken when the surface structure of $\sqrt{21}$-Cs is formed. This is consistent with the above-mentioned conclusion from STM observations.

The question left to answer is what causes the difference between Cs and noble-metal induced $\sqrt{21} \times \sqrt{21}$ phases. In the cases of $\sqrt{21}$-Au and $\sqrt{21}$-Ag phases, Tong *et al.* have suggested that Au or Ag adatoms act as a kind of perturbation to the initial $\sqrt{3} \times \sqrt{3}$-Ag surface;[3)] the adatoms dope electrons into the surface-state bands of the initial $\sqrt{3} \times \sqrt{3}$-Ag surface to make the bands shift downwards, and to make a kind of ionic surface boding between the adatoms and substrate. The adatoms are partly ionised positively, leading to a repulsive interaction among the adatoms. Since Cs atoms have larger electronegativity than Au and Ag atoms, such charge transfer and Coulomb repulsions among adatoms might be larger. This might lead to a total breakdown of the initial $\sqrt{3} \times \sqrt{3}$-Ag framework and induce a new reconstruction by Cs adsorption. The atomic radius is also quite different between Cs (0.266 nm) and Au/Ag (0.144 nm),[15)] which can be another reason for the difference. Bonding energies of Si–Ag and Si–Cs can also be an important factor to determine whether Ag atoms in the initial $\sqrt{3} \times \sqrt{3}$-Ag surface are replaced by Cs atoms.

4. Conclusion

Evaporating Cs atoms onto the Si(111)-$\sqrt{3} \times \sqrt{3}$-Ag surface at RT induced the $\sqrt{21}$-Cs phase as in the cases of noble-metal depositions. However the STM images of the $\sqrt{21}$-Cs surface looked completely different from those of the $\sqrt{21}$-Ag and $\sqrt{21}$-Au surfaces, indicating that the Cs induced $\sqrt{21} \times \sqrt{21}$ phase should have its own atomic structure different from that of noble-metal induced $\sqrt{21} \times \sqrt{21}$. In addition, the ARPES data showed that the surface-state bands of the $\sqrt{21}$-Cs phase were also totally different from those of the $\sqrt{21}$-Ag and $\sqrt{21}$-Au surfaces. This is another important evidence to show that Cs induced $\sqrt{21} \times \sqrt{21}$ phase is different from the Ag or Au induced one. There seemed no traces of the framework of Si(111)-$\sqrt{3} \times \sqrt{3}$-Ag structure remaining in the $\sqrt{21}$-Cs phase. More studies including theoretical ones are needed to obtain the details of the atomic and electronic structures.

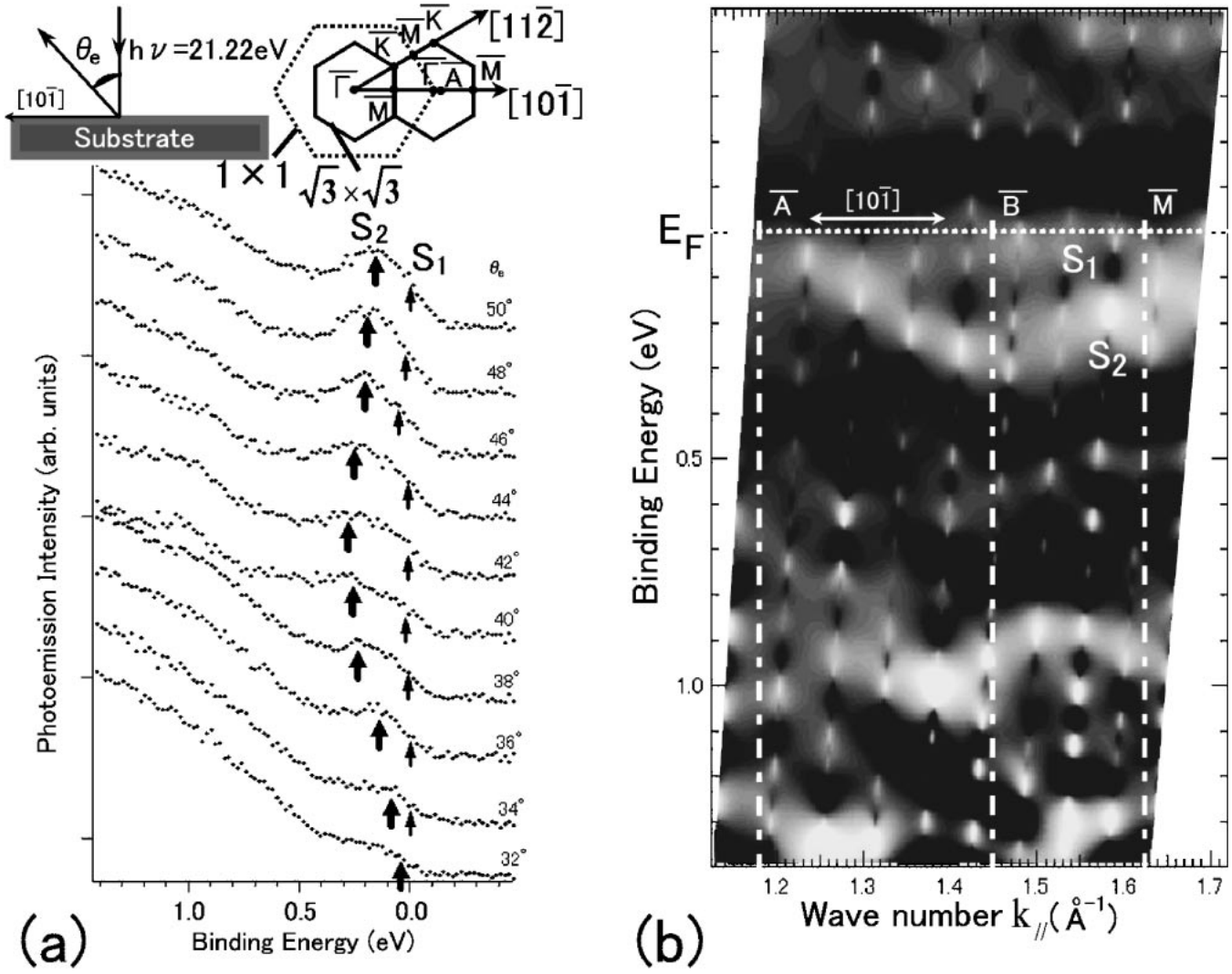

Fig. 4. (a) ARPES spectra and (b) gray-scale band-dispersion diagram for the Si(111)-$\sqrt{21}\times\sqrt{21}$-(Ag+Cs) surface, respectively. The incident synchrotron beam is normal to the surface, and the emitted photoelectrons were detected in the plane defined by the directions of [111] and [10$\bar{1}$], so that a part of the gray-scale band-dispersion alone [10$\bar{1}$] is compiled using the second derivatives of the original spectra. $\bar{\mathbf{A}}$ and $\bar{\mathbf{M}}$ in (b) correspond to those in the insertion of Brilliouin zones in (a).

Acknowledgments

Helpful advise on degassing the source of Caesium from Professor Patrick Soukiassian and Dr. Marie D'angelo is acknowledged. We thank Mr. Takehiro Tanikawa, Mr. Rei Hobara and Mr. Mitsuru Konishi for their support and assistance with the experiments.

1) J. Nogami, K. J. Wan and X. F. Lin: Surf. Sci. **306** (1994) 81.
2) A. Ichimiya, H. Nomura, Horio, T. Sato, T. Sueyoshi and M. Iwatsuki: Surf. Rev. Lett. **1** (1994) 1.
3) X. Tong, C. S. Jiang and S. Hasegawa: Phys. Rev. B **57** (1998) 9015.
4) H. Tajiri, K. Sumitani, W. Yashiro, S. Nakatani, T. Takahashi, K. Akimoto, H. Sugiyama, X. Zhang and H. Kawata: Surf. Sci. **493** (2001) 214.
5) S. Hasegawa, X. Tong, S. Takeda, N. Sato and T. Nagao: Prog. Surf. Sci. **60** (1999) 89.
6) X. Tong, Y. Sugiura, T. Nagao, T. Takami, S. Takeda, S. Ino and S. Hasegawa: Surf. Sci. **408** (1998) 146.
7) X. Tong, S. Ohuchi, N. Sato, T. Tanikawa, T. Nagao, I. Matsuda, Y. Aoyagi and S. Hasegawa: Phys. Rev. B **64** (2001) 205316.
8) X. Tong, S. Ohuchi, T. Tanikawa, A. Harasawa, T. Okuda, Y. Aoyagi, T. Kinoshita and S. Hasegawa: Appl. Surf. Sci. **190** (2002) 121.
9) C.-S. Jiang, X. Tong and S. Hasegawa: Surf. Sci. **376** (1997) 69.
10) X. Tong, S. Hasegawa and S. Ino: Phys. Rev. **B55** (1997) 1310.
11) X. Tong, C. S. Jiang, K. Horikoshi and S. Hasegawa: Surf. Sci. **449** (2000) 125.
12) Y. Nakajima, S. Takeda, T. Nagao, S. Hasegawa and X. Tong: Phys. Rev. **B56** (1997) 6782.
13) T. Takahashi, S. Nakatani, N. Okamoto, T. Ichikawa and S. Kikuta: Jpn. J. Appl. Phys. **27** (1988) L753.
14) H. Aizawa and M. Tsukada: Phys. Rev. **B59** (1999) 10923.
15) *Periodic Table of the Elements*, eds. Fluck and Heumann with IUPAC recommendations of 1999 (WILEY-VCH, Verlag GmbH, 1999) 2nd ed.